Digitization and Visibility Issues in Flat Detector CT: A Simulation Study

Michael Knaup[1], Ludwig Ritschl[1], and Marc Kachelrieß[1,2]

[1]Institute of Medical Physics, University of Erlangen-Nürnberg, Germany

[2]Medical Physics in Radiology, German Cancer Research Center (DKFZ), Heidelberg, Germany

Introduction:

Flat detector CT suffers from a limited visibility of low-contrast objects. On the one hand this is due to increased image noise and x-ray scatter, on the other hand this can be attributed to a limited dynamic range of current flat detectors. Compared to clinical CT detectors with their energy absorption efficiency of 90% or more and their dynamic range of 20 bits or more, flat detectors with their energy absorption efficiency around 50 or 60% and their dynamic range of 10 to 12 bits above the noise floor [1] are significantly inferior. Further on, often intended or unintended over- or underexposure occurs in flat detector CT systems, resulting in undesired effects on image quality. To explore the situation we conduct a simulation study that systematically analyzes the effects of limited dynamic range and of over- or underexposure on CT image quality in general and on low-contrast visibility in particular.

Simulation:

We performed simulations in 2D parallel beam geometry with 512 projection angles ϑ and 512 rays ξ per projection. Prior to the reconstruction with a standard filtered backprojection algorithm, the ideal line integrals $p(\vartheta,\xi)$ obtained from those simulations will be manipulated in the following steps:

1. Relative Intensities

$$q_0(\vartheta,\xi) = e^{-p(\vartheta,\xi)}$$

2. Scaling Factor s

$$q_1 = q_0^s$$

3. Quantum Noise

$$q_2 = q_1 + \mathcal{N}\sqrt{q_1/I_0}$$

$\mathcal{N}$: Gaussian distributed random number with mean 0 and standard deviation 1.

I_0 : Number of detected quanta for the zero image.

4. Gain Factor g

$$q_3 = g\, q_2$$

5. AD Conversion and Saturation

$$q_4 = q_3 + \mathcal{U}\, 2^{-b}$$

$$q_5 = \varepsilon \vee \frac{\lfloor q_4(2^b-1)+\frac{1}{2}\rfloor}{2^b-1} \wedge 1$$

$\mathcal{U}$: Uniformly distributed random number in the interval $[-\frac{1}{2},\frac{1}{2}]$.

b : Effective number of significant bits.

$\varepsilon = \frac{1}{2}(2^b-1)^{-1}$

Generation of ideal phase steps

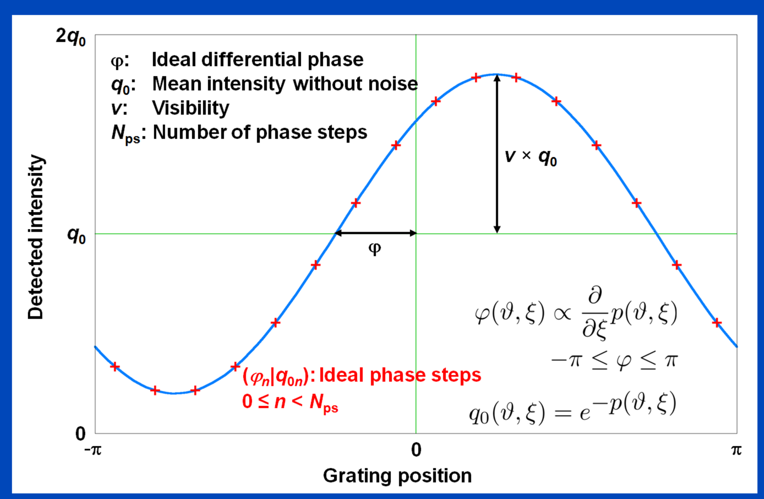

Fig. 1: Ideal phase steps $(\varphi_n|q_{0n})$ are generated from simulated line integrals $p(\vartheta,\xi)$. The visibility was set to a reasonable constant value v = 0.3 [2].

Determination of the noisy phase

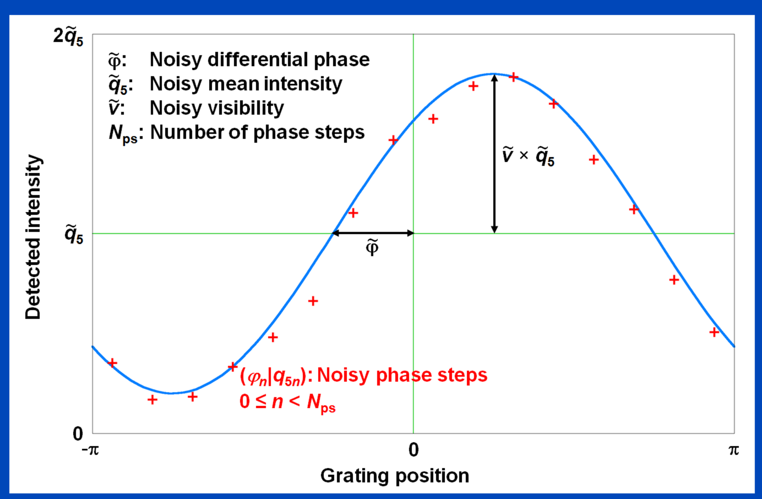

Fig. 2: Noisy phase steps are generated by applying steps 2 to 5 to the ideal phase steps q_{0n}. The noisy differential phase, mean intensity, and visibility are then determined by a least square fit.

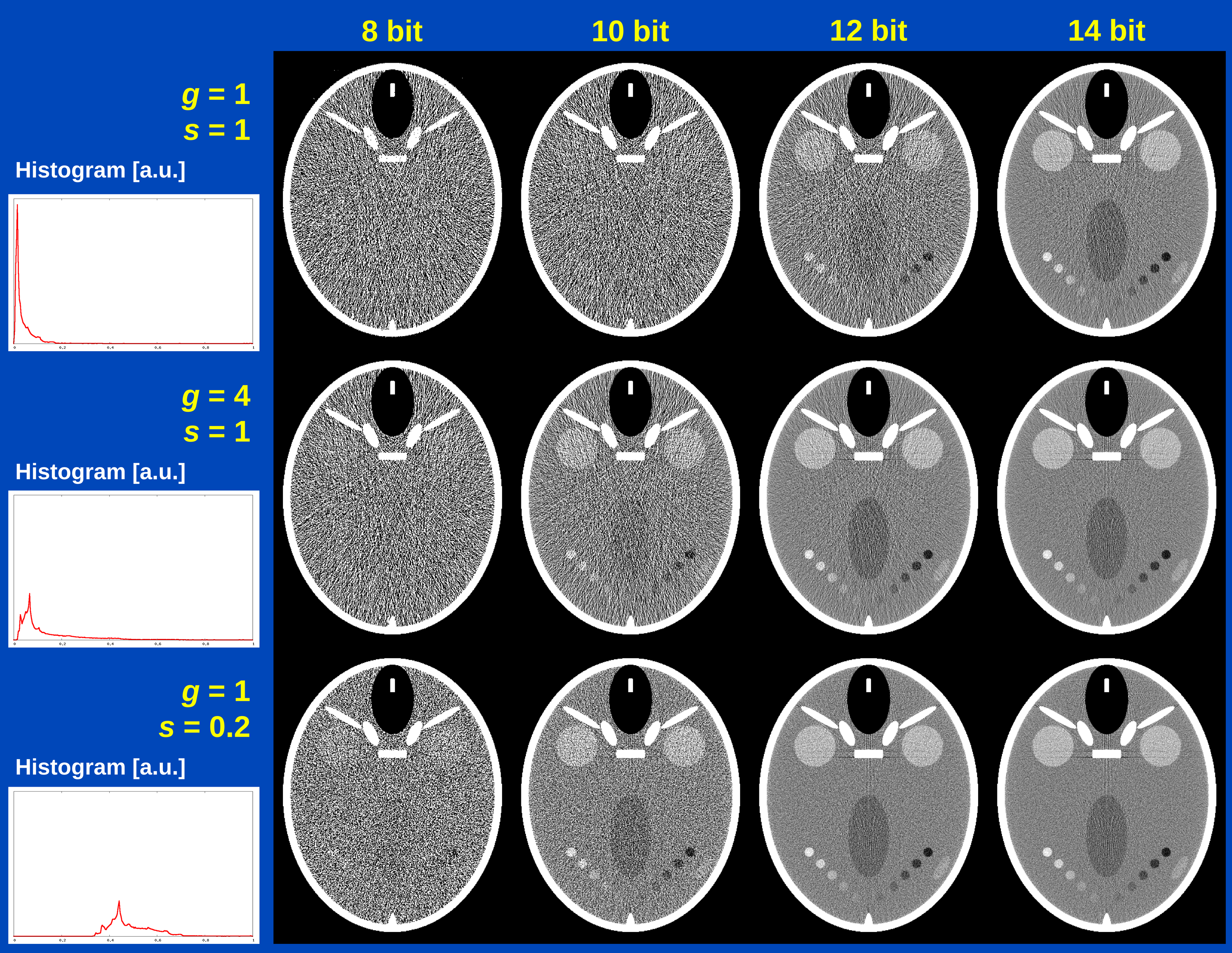

Fig. 3: Attenuation based reconstructions of a modified Forbild head phantom [3]. Top row: Gain g = 1, scale s = 1 (standard exposure, patient imaging). Middle row: g = 4, s = 1 (intended overexposure, patient imaging). Bottom row: g = 1, s = 0.2 (standard exposure, small animal imaging). Histograms are generated from the analog signal q_0. $I_0 = 2.7\times10^7$. (C/W) = (50/50).

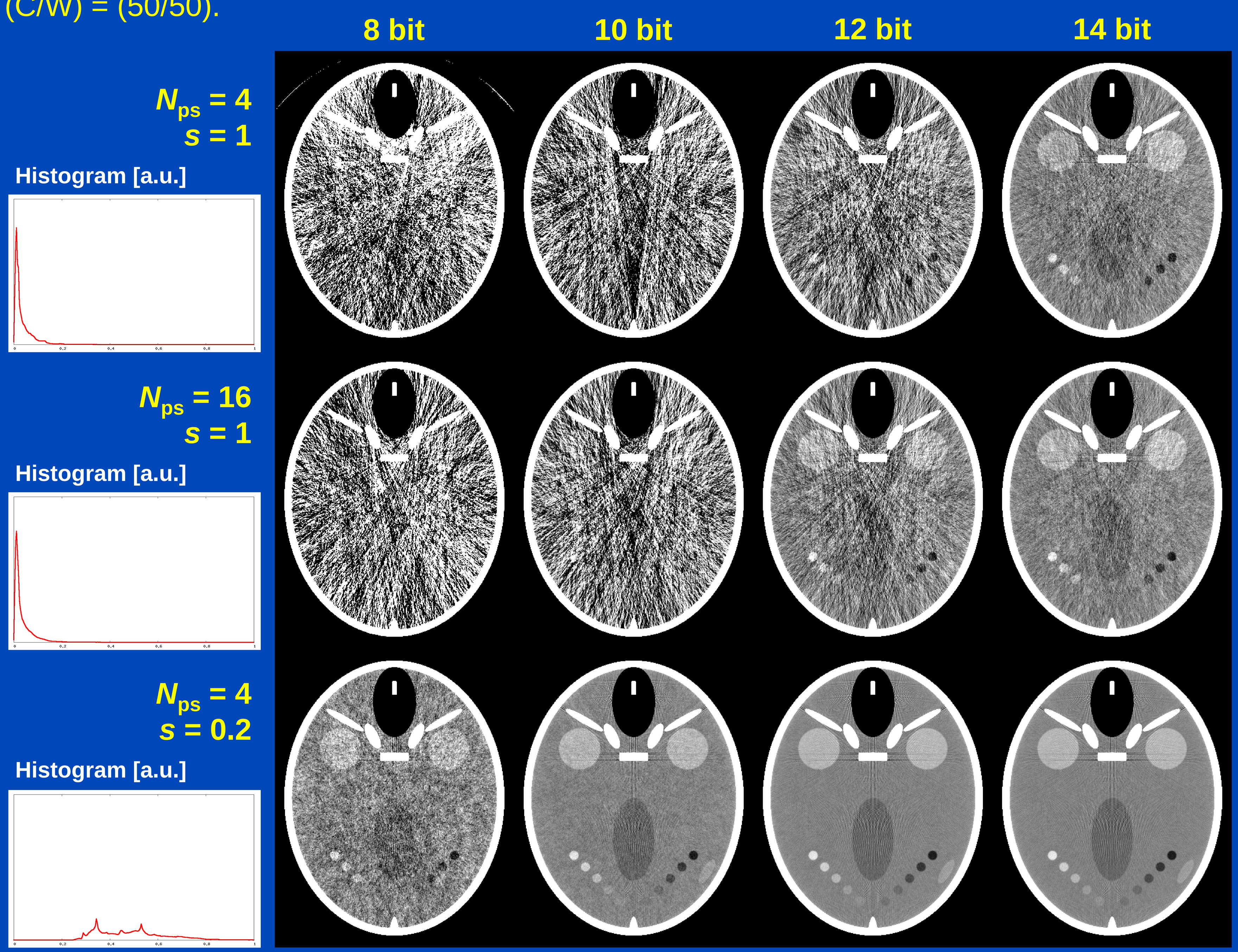

Fig. 4: Differential phase-contrast reconstructions of a modified Forbild head phantom [3]. Top row: N_{ps} = 4 phase steps, scale s = 1. Middle row: N_{ps} = 16, s = 1. Bottom row: N_{ps} = 4, s = 0.2. All rows: Gain g = 1. Histograms are generated from the ideal phase steps q_{0n}. $I_0 = 2.7\times10^7 / N_{ps}$, i.e. equal dose for each image. (C/W) = (50/50).

6. Logarithm

$$p_6 = \begin{cases} 0 & \text{if } q_5 = 1 \\ -\ln(q_5/g) & \text{if } q_5 < 1 \end{cases}$$

Grating-based differential phase-contrast imaging

The simulations were also used to generate noisy differential phases (see figs. 1 and 2). Images were reconstructed as described in ref. [2].

Results:

Figs. 3 and 4 show results for a modified Forbild head phantom [3].

For attenuation-based imaging it is interesting to see that the images that are overexposed by a factor of g = 4 taken with b true bits are comparable to the images without overexposure taken at b+2 bits.

It is also interesting to see, that for both imaging methods the change in scale by a factor of five results in significantly different images. While the large patient data require a higher detector dynamic range, the small animal size data can do with less bits.

Summary and Conclusions:

We analyzed and demonstrated the influence of detector quantization on low contrast detectability for both attenuation CT and differential phase-contrast CT imaging.

For attenuation-based imaging, intended overexposure of the detector can improve the low-contrast detectability in certain situations.

Imaging on the scale of small animals requires a lower dynamic detector range than imaging on the larger scale of a patient. This might be utilized by applying an analog gamma amplifier prior to digitalization for patient imaging.

Acknowledgments:

This work was supported by the Deutsche Forschungsgemeinschaft under grant FOR 661. The reconstruction software was provided by RayConStruct® GmbH, Nürnberg, Germany.

References:

[1] P. G. Roos et al., "Multiple gain ranging readout method to extend the dynamic range of amorphous silicon flat panel imagers," *SPIE Medical Imaging Proc., vol. 5368, pp. 139–149,* 2004.

[2] R. Raupach and T. Flohr, "Analytical evaluation of the signal and noise propagation in x-ray differential phase-contrast computed tomography," *Physics in Medicine and Biology, vol. 56, pp. 2219–2244, 2011.*

[3] www.imp.uni-erlangen.de/phantoms.

Send correspondence request to:

Dr. Michael Knaup
michael.knaup@imp.uni-erlangen.de

Institute of Medical Physics
Friedrich-Alexander-University (FAU)
Henkestr. 91, 91052 Erlangen,Germany